

Russell B. Kidman and Arthur N. Cox  
 Theoretical Division, Los Alamos National Laboratory  
 University of California  
 Los Alamos, NM 87544

In this paper we discuss the decay rate for many of the low degree  $p$  modes observed as 5 minute oscillations of the sun. This report is an expanded version of the presentation at Snowmass. These theoretical results use the completely nonadiabatic linear theory of Saio and Cox (1980). Our solar model is based on the evolution results of Christensen-Dalsgaard (1982). Equation of state and opacity data come from the Los Alamos Opacity Library of Huebner, Merts, Magee, and Argo (1977). We compute decay rates for modes ranging from radial ( $\ell=0$ ) to the nonradial ones with  $\ell=5$  for overtones 10 through 28.

Parameters needed for our solar model are given in Table 1. Figure 1 shows the hydrogen mass fraction composition structure. Also given on the figure is the structure given by Christensen-Dalsgaard (1982) for an evolved solar model. Our special equation of state and opacity table with  $X=0.74$  for the hydrogen mass fraction in the outer 0.40 of the mass needs slightly more hydrogen in the central regions than obtained by Christensen-Dalsgaard in order to give a complete and consistent model. The difference in helium production between these two models is about 10%, meaning that the total energy radiated by the sun during its lifetime thus far agrees satisfactorily with accurately calculated evolution sequences.

TABLE 1

## SOLAR MODEL:

Luminosity	$3.90 \times 10^{33}$ erg sec <sup>-1</sup>
Mass	$1.989 \times 10^{33}$ g
Radius	$6.955 \times 10^{10}$ cm
Surface temperature	$5.8 \times 10^3$ K
Central temperature	$1.51 \times 10^7$ K
Central density	$122.3$ g cm <sup>-3</sup>
Surface X, Y, Z	0.740, 0.240, 0.020
Central X, Y, Z	0.450, 0.530, 0.020
Depth of convection zone	$0.32R_{\odot}$ ( $0.043M_{\odot}$ )
Temp. at bot. of convec. zone	$2.50 \times 10^6$ K
Central ball	$0.05R_{\odot}$ ( $0.01M_{\odot}$ )
Surface-zone mass	$3.0 \times 10^{22}$ g

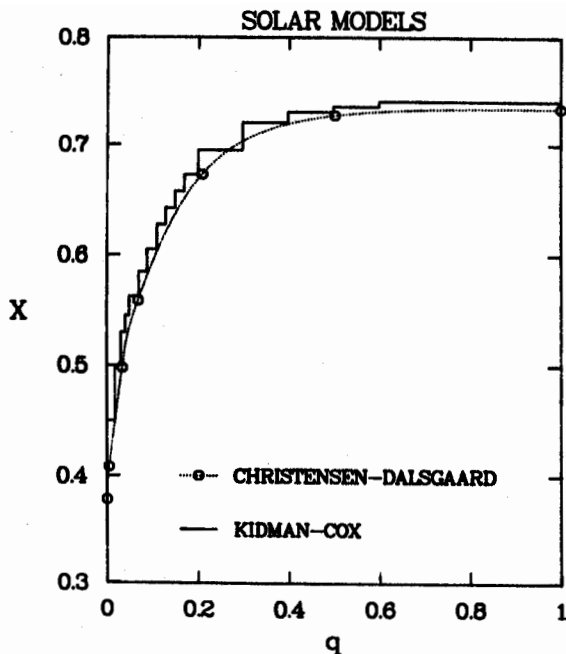


Figure 1. The hydrogen mass fraction of the composition,  $X$ , is plotted versus interior mass fraction of the solar model.

Figure 2 is a plot of the logarithms of temperature (K), opacity ( $\text{cm}^2/\text{g}$ ), and density ( $\text{g}/\text{cm}^3$ ) for our model versus the logarithm of the exterior mass. The very high opacity over the outer 4% of the mass produces a very deep convection zone. The rapid rise of temperature just cooler than 7,000 K requires a small density inversion to give the proper run of pressure to maintain hydrostatic balance. The ratio of mixing length to pressure scale height for all the convection zone is 1.5.

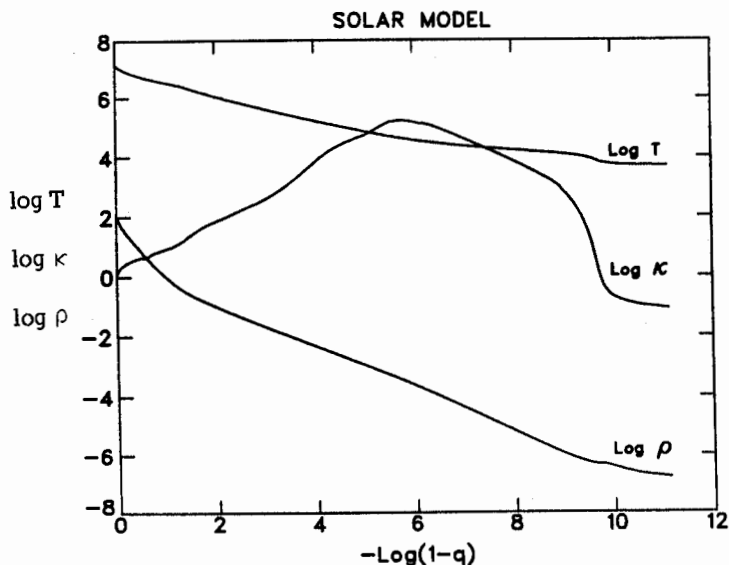


Figure 2. The temperature, opacity, and density structure of the sun is plotted versus the logarithm of the exterior mass fraction.

Solution for the eigenvalues and eigenvectors for the nonradial modes is made for all six of the Dziembowski (1971) variables which have both real and imaginary parts. Figure 3 gives the central variations of  $y_1$ , the Lagrangian variation of the mass shells in the radial direction. The imaginary part, which indicates the variation structure at the mean radius phase of the pulsation as contrasted with the real part applying to the time of the maximum expansion for these linear sinusoidal motions, is very small. This means that the oscillations for this  $p_{23}$ ,  $\ell=2$  mode are very adiabatic. There is little phase change for these lobes which gives essentially standing rather than running waves. Figures 4 and 5 give this same radial variation structure in the outer

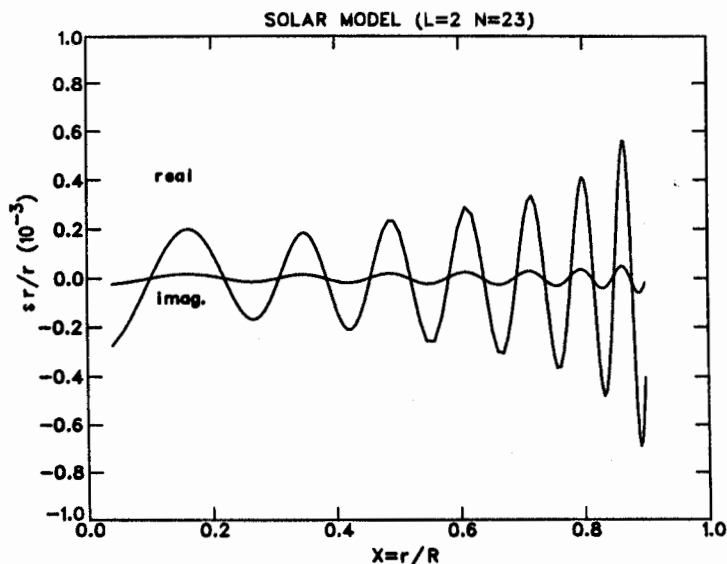


Figure 3. The central variations of the real and imaginary parts of the radial component of the  $p_{23}$ ,  $\ell=2$  oscillations are plotted versus radius fraction. At  $x=0.2$ , 30% of the solar mass is interior. Only 6% of the mass is interior to  $x=0.1$ . At  $x=0.4$  the interior mass is 75% of the model mass.

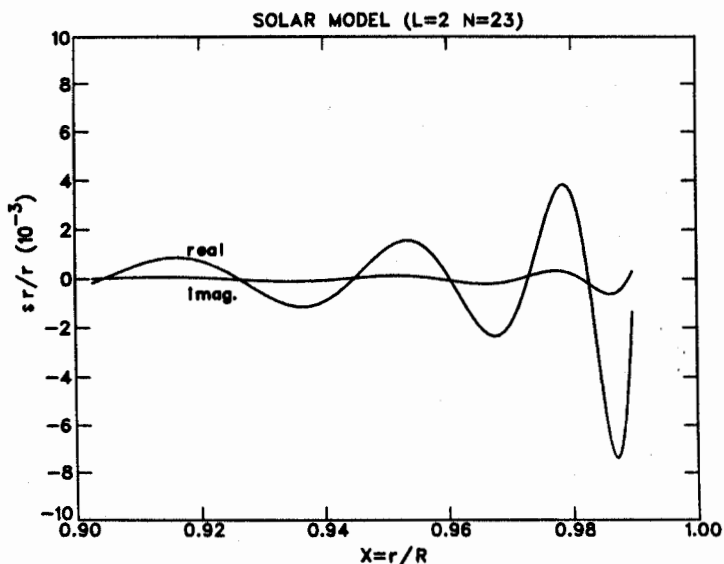


Figure 4. The radial component real and imaginary parts of the  $p_{23}$ ,  $\ell=2$  oscillations are plotted for the outer 10% of the radius.

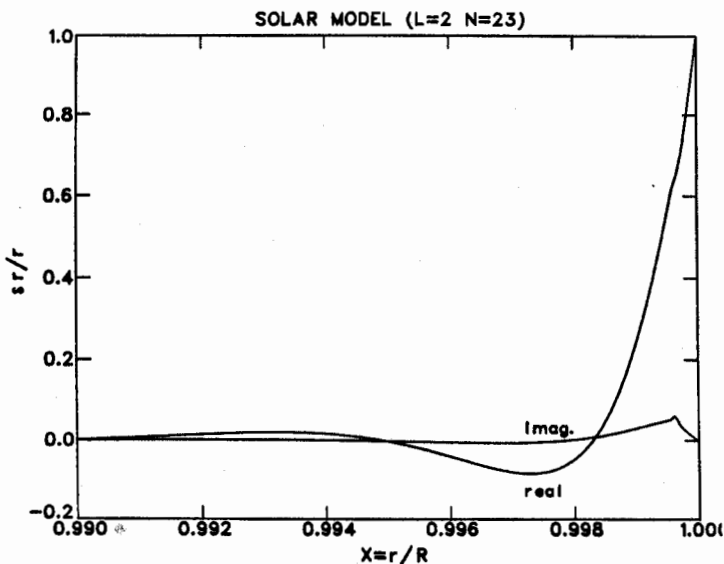


Figure 5. The radial component real and imaginary parts of the  $p_{23}$ ,  $l=2$  oscillations are plotted for the outer 1% of the radius.

10% and 1% of the radius. Only at the surface is there any phase change of the real and imaginary parts of this variation, and there also is a significant nonadiabatic effect. At the very surface, the usual normalization gives unity for the real part and zero for the imaginary part. Damping of this mode is related to this feature of the eigensolution, and it is discussed below using the derived complex eigenvalue.

Periods for many modes are given in Tables 2 to 7, respectively, for  $l=0$  to 5. Modes  $p_{10}$  to  $p_{28}$  frequencies are listed together with the frequencies observed by Harvey and Duvall (1983). The listed periods and frequencies are from the adiabatic solutions, and the few  $\mu\text{Hz}$  corrections to get the nonadiabatic periods are also given for each mode. Decay rates are calculated by taking the ratio of the imaginary and real parts of the eigenvalue and multiplying this ratio by  $4\pi$ . It is also possible to integrate the P-V loops that all these Lagrangian zones traverse each cycle to get the work done by or done on these zones each cycle. The sum over all the mass zones agrees well with the decay rate derived directly from the eigenvalue component ratio. For each mode the decay times are given in terms of the number of cycles and in terms of the real time.

Our calculations were done with only 329 mass shells and the central ball. These 330 zones are not quite enough to define well the eigensolutions, and we get frequencies 1.3 to 2.5% too large compared with the observed frequencies. See Figure 6 where a comparison of our frequencies with those of Shibahashi et al. (essentially the observed ones) is made. This trend indicates a zoning error, because it decreases with increasing resolution of the pulsation mode and its eigensolutions. Our optimum zoning has very fine mass shells down to a depth of 3.5 million kelvin. In this outer region the temperature increases only about 3% per zone. In the deeper layers, the 100 more zones have a mass ratio from zone to zone of 1.003. We estimate maybe 100 more carefully placed zones could give adequately accurate periods. Our actual

frequencies should not be accepted for high accuracy, but the decay rates listed in the tables should be well determined.

TABLE 2

periods, frequencies and decay rates

l	n	period (sec)	adiabatic frequency (uhz)	non-a incre (uhz)	measured frequency (uhz)	decay by e	
						number of cycles	time (days)
0	10	620.895	1610.6	-15.50	0.0	18330.7	131.73
0	11	573.397	1744.0	-11.97	0.0	8378.6	55.61
0	12	532.832	1876.8	-9.62	0.0	4294.2	26.48
0	13	497.510	2010.0	-8.13	0.0	2481.6	14.29
0	14	466.240	2144.8	-6.83	0.0	1483.9	8.01
0	15	438.540	2280.3	-5.92	0.0	933.4	4.74
0	16	414.175	2414.4	-5.01	0.0	607.0	2.91
0	17	392.092	2550.4	-4.34	0.0	429.3	1.95
0	18	372.124	2687.3	-3.99	0.0	330.4	1.42
0	19	354.083	2824.2	-3.75	0.0	269.5	1.10
0	20	337.481	2963.1	-3.56	0.0	227.6	.89
0	21	322.317	3102.5	-3.41	0.0	191.9	.72
0	22	308.399	3242.6	-3.30	0.0	167.0	.60
0	23	295.583	3383.1	-3.19	0.0	144.7	.50
0	24	283.583	3526.3	-3.16	0.0	132.0	.43
0	25	272.492	3669.8	-3.24	0.0	120.6	.38
0	26	262.244	3813.2	-3.39	0.0	109.4	.33
0	27	252.677	3957.6	-3.48	0.0	105.4	.31
0	28	243.731	4102.9	-3.70	0.0	97.7	.28
x							

TABLE 3

periods, frequencies and decay rates

l	n	period (sec)	adiabatic frequency (uhz)	non-a incre (uhz)	measured frequency (uhz)	decay by e	
						number of cycles	time (days)
1	10	607.745	1645.4	-.58	0.0	13601.4	95.67
1	11	560.942	1782.7	-.59	0.0	6376.5	41.40
1	12	521.033	1919.3	-.54	0.0	3384.0	20.41
1	13	486.203	2056.8	-.54	0.0	1994.7	11.22
1	14	455.839	2193.8	-.58	2161.0	1217.2	6.42
1	15	428.930	2331.4	-.66	2293.0	765.3	3.80
1	16	405.383	2466.8	-.80	2427.0	526.7	2.47
1	17	384.277	2602.3	-.93	0.0	385.9	1.72
1	18	365.017	2739.6	-1.09	0.0	300.8	1.27
1	19	347.465	2878.0	-1.26	2828.0	251.2	1.01
1	20	331.336	3018.1	-1.48	2962.0	211.3	.81
1	21	316.638	3158.2	-1.73	3098.0	180.4	.66
1	22	303.087	3299.4	-2.02	3233.0	157.3	.55
1	23	290.779	3439.0	-2.29	3368.0	142.0	.48
1	24	279.264	3580.8	-2.55	3506.0	128.5	.42
1	25	268.522	3724.1	-2.86	3641.0	116.4	.36
1	26	258.625	3866.6	-3.14	3779.0	108.0	.32
1	27	249.252	4012.0	-3.41	3917.0	102.7	.30
1	28	240.563	4156.9	-3.75	4058.0	95.8	.27
x							

TABLE 4

periods, frequencies and decay rates

l	n	period (sec)	adiabatic frequency (uhz)	non-a incre (uhz)	measured frequency (uhz)	decay by e	
						number of cycles	time (days)
2	10	588.804	1698.4	.41	0.0	9961.5	67.89
2	11	544.902	1835.2	.34	0.0	4913.6	30.99
2	12	507.211	1971.6	.30	0.0	2740.5	16.09
2	13	473.968	2109.8	.26	2083.0	1620.9	8.89
2	14	444.909	2247.7	.22	2222.0	1009.5	5.20
2	15	419.299	2384.9	.12	2352.0	642.2	3.12
2	16	396.417	2522.6	-.00	2487.0	452.1	2.07
2	17	375.999	2659.6	-.14	2620.0	345.4	1.50
2	18	357.558	2796.7	-.32	2757.0	277.6	1.15
2	19	340.615	2935.9	-.51	2890.0	234.3	.92
2	20	325.108	3075.9	-.74	3024.0	196.9	.74
2	21	310.911	3216.4	-1.00	3161.0	170.4	.61
2	22	297.790	3358.1	-1.31	3295.0	147.1	.51
2	23	285.664	3500.6	-1.57	0.0	135.2	.45
2	24	274.496	3643.0	-1.87	3567.0	123.6	.39
2	25	264.189	3785.2	-1.54	3703.0	111.8	.34
2	26	254.538	3928.7	-2.52	3840.0	107.1	.32
2	27	245.479	4073.7	-2.92	3980.0	99.4	.28
2	28	237.019	4219.1	-3.32	0.0	92.8	.25

TABLE 5

periods, frequencies and decay rates

l	n	period (sec)	adiabatic frequency (uhz)	non-a incre (uhz)	measured frequency (uhz)	decay by e	
						number of cycles	time (days)
3	10	571.766	1749.0	-.12	0.0	7467.2	49.42
3	11	529.913	1887.1	-.07	0.0	3847.3	23.60
3	12	493.873	2024.8	-.07	0.0	2235.7	12.78
3	13	462.340	2162.9	-.08	0.0	1340.2	7.17
3	14	434.513	2301.4	-.12	0.0	840.4	4.23
3	15	410.225	2437.7	-.18	2408.0	559.8	2.66
3	16	388.319	2575.2	-.29	2542.0	400.9	1.80
3	17	368.460	2714.0	-.42	2677.0	310.6	1.32
3	18	350.527	2852.8	-.56	2812.0	257.3	1.04
3	19	334.074	2993.3	-.74	2948.0	217.1	.84
3	20	319.106	3133.8	-.95	3082.0	184.4	.68
3	21	305.351	3274.9	-1.19	3219.0	161.0	.57
3	22	292.805	3415.2	-1.47	3354.0	142.5	.48
3	23	281.019	3558.5	-1.75	3491.0	129.1	.42
3	24	270.083	3702.6	-2.05	3628.0	117.7	.37
3	25	260.026	3845.8	-2.39	3763.0	108.2	.33
3	26	250.565	3991.0	-2.47	3904.0	103.9	.30
3	27	241.792	4135.8	-3.00	0.0	96.7	.27
3	28	233.600	4280.8	-3.38	0.0	90.9	.25

TABLE 6

periods, frequencies and decay rates

l	n	period (sec)				decay by e	
			adiabatic frequency (uhz)	non-a incre (uhz)	measured frequency (uhz)	number of cycles	time (days)
4	10	557.147	1794.9	-.32	0.0	5860.3	37.79
4	11	517.054	1934.0	-.25	1918.0	3126.2	18.71
4	12	482.165	2074.0	-.22	2052.0	1838.4	10.26
4	13	451.906	2212.8	-.24	0.0	1125.7	5.89
4	14	425.186	2351.9	-.29	0.0	706.5	3.48
4	15	401.713	2489.3	-.37	2323.0	490.8	2.28
4	16	380.754	2626.4	-.49	2459.0	364.8	1.61
4	17	361.671	2764.9	-.62	0.0	286.6	1.20
4	18	344.215	2905.2	-.77	2728.0	240.6	.96
4	19	328.227	3046.7	-.95	2866.0	201.9	.77
4	20	313.662	3188.1	-1.18	3000.0	173.6	.63
4	21	300.227	3330.8	-1.44	3138.0	150.5	.52
4	22	287.973	3472.5	-1.68	3272.0	137.9	.46
4	23	276.614	3615.1	-1.96	3409.0	125.2	.40
4	24	266.021	3759.1	-2.31	3545.0	112.9	.35
4	25	256.241	3902.6	-2.58	3683.0	106.7	.32
4	26	246.976	4049.0	-2.91	3821.0	99.9	.29
4	27	238.372	4195.1	-3.29	3962.0	93.4	.26
4	28	230.338	4341.4	-3.65	0.0	88.4	.24

TABLE 7

periods, frequencies and decay rates

l	n	period (sec)				decay by e	
			adiabatic frequency (uhz)	non-a incre (uhz)	measured frequency (uhz)	number of cycles	time (days)
5	10	543.763	1839.0	-.37	0.0	4739.6	29.83
5	11	505.486	1978.3	-.31	1963.0	2621.0	15.33
5	12	471.871	2119.2	-.28	2100.0	1541.7	8.42
5	13	442.601	2259.4	-.30	2235.0	957.2	4.90
5	14	416.968	2398.3	-.36	2371.0	612.0	2.95
5	15	394.088	2537.5	-.45	2505.0	432.6	1.97
5	16	373.676	2676.1	-.58	2641.0	332.0	1.44
5	17	355.271	2814.8	-.74	2777.0	268.6	1.10
5	18	338.341	2955.6	-.89	2914.0	226.2	.89
5	19	322.877	3097.2	-1.10	3050.0	190.1	.71
5	20	308.710	3239.3	-1.32	3187.0	165.1	.59
5	21	295.690	3381.9	-1.61	3324.0	143.3	.49
5	22	283.586	3526.3	-1.85	3460.0	131.4	.43
5	23	272.457	3670.3	-2.14	3597.0	120.3	.38
5	24	262.192	3814.0	-2.49	3733.0	109.3	.33
5	25	252.612	3958.6	-2.73	3871.0	105.2	.31
5	26	243.644	4104.3	-3.11	0.0	97.4	.27
5	27	235.256	4250.7	-3.48	0.0	91.0	.25
5	28	227.276	4399.9	-5.83	0.0	86.0	.23

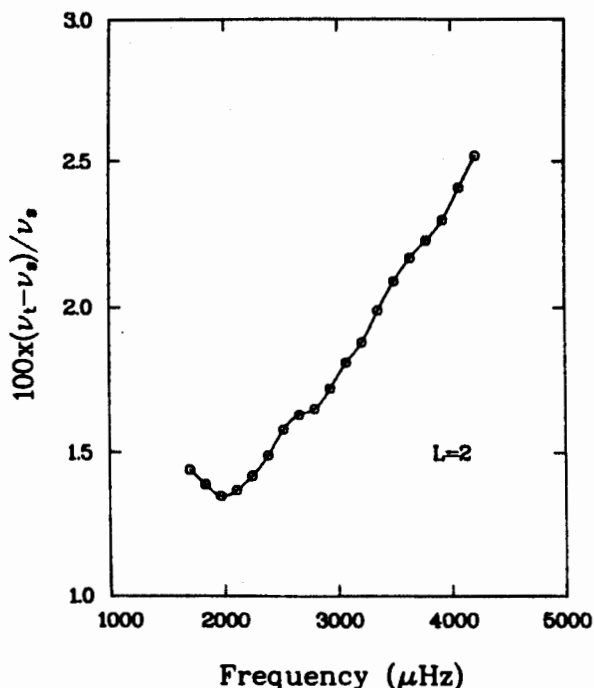


Figure 6. The mode frequency error, as judged from the Shibahashi et al. values, is plotted versus the mode frequency.

A comparison with observations seems to show reasonable agreement with our predictions. The width of the peaks in the power spectrum indicates a decay rate, which is perhaps a matter of days. The coherence of modes over timescales of a month or longer might mean that the mode is reexcited in its existing phase, or it might refer merely to our predicted longer lived modes. Decay rates are faster for higher frequencies because they refer to smaller-scale structures which can more easily gain and lose energy during an oscillation.

Figure 7 shows the work over each pulsation cycle for the outer 30 zones down to a depth of 12,000 K. Actually, the opacity library does not give data for such low temperatures, and the opacities and equation of state are obtained over this region by use of the Stellingwerf (1975ab) analytic fit. The photospheric damping, always assuming a radiation diffusion structure, down to depths of about 40 Rosseland mean opacity mean free paths is the main damping of the solar oscillations. Zone 317 is at  $\tau=10$ , zone 319 is at  $\tau=5$  and zone 324 is at  $\tau=1$ . At least half of the damping occurs where our diffusion approximation is valid. The  $\gamma$  and  $\kappa$  effects of the hydrogen ionization region give some deeper pulsation driving, but it is not enough to self-excite the solar oscillations. The convection zone is neutral because we assume, as is usually done, that the convective flux is frozen at its equilibrium value. Deeper than 10,000 K the very small radiative flux is still modulated, but no more hydrogen or helium driving is significant.

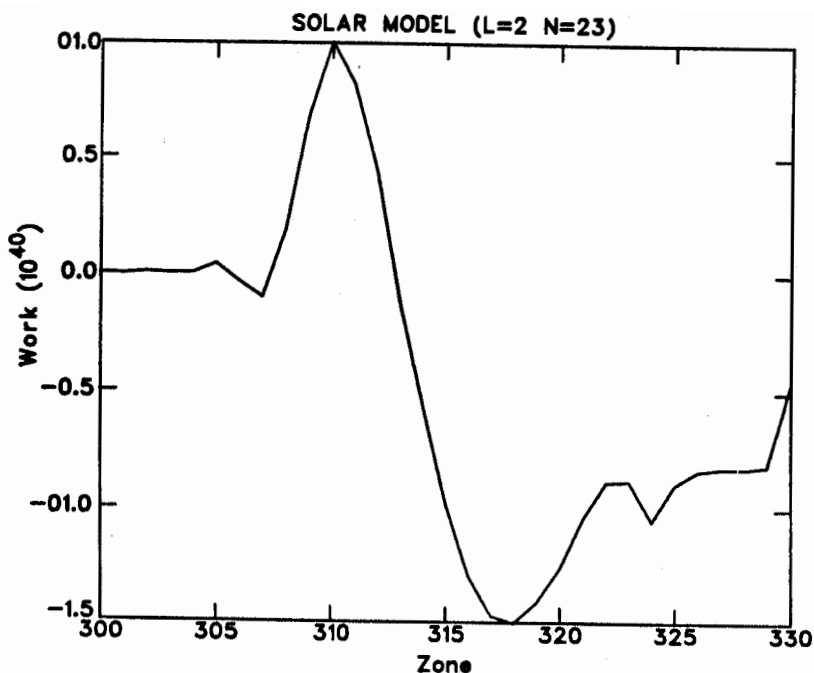


Figure 7. Damping and driving regions of the surface layers are plotted for the outermost 30 zones.

Our conclusions are that all solar 5-minute modes of low order are damped with widely varying rates which increase with frequency. These nonadiabatic effects are confined to the outer  $5 \times 10^{-10}$  of the mass and the outer  $3 \times 10^{-4}$  of the radius.

#### References

- Christensen-Dalsgaard, J. 1982 M.N.R.A.S. 199, 735.  
 Dziembowski, W. 1971 Acta Ast. 21, 289.  
 Harvey, J. and Duvall T. 1983 this conference.  
 Huebner, W.F., Merts, A.L., Magee, N.H., and Argo, M.F. 1977 Los Alamos Scientific Laboratory report LA-6760-M.  
 Saio, H. and Cox, J.P. 1980, Ap.J. 236, 549.  
 Shibahash:, H., Noels, A., and Gabriel, M. 1983, Astron. Ap. 123,283.  
 Stellingwerf, R.F. 1975a, Ap.J. 195, 441.  
 Stellingwerf, R.F. 1975b, Ap. J. 199, 705.